

# Extended Hubble Diagram on the Basis of Gamma Ray Bursts Including the High Redshift Range of $z = 0.0331 - 8.1$

Laszlo A. Marosi

Ludwigshafen am Rhein, Germany

Email: LaszloMarosi@aol.com

**How to cite this paper:** Marosi, L.A. (2019) Extended Hubble Diagram on the Basis of Gamma Ray Bursts Including the High Redshift Range of  $z = 0.0331 - 8.1$ . *International Journal of Astronomy and Astrophysics*, 9, 1-11.

<https://doi.org/10.4236/ijaa.2019.91001>

**Received:** November 17, 2018

**Accepted:** January 21, 2019

**Published:** January 24, 2019

Copyright © 2019 by author(s) and Scientific Research Publishing Inc.

This work is licensed under the Creative Commons Attribution International License (CC BY 4.0).

<http://creativecommons.org/licenses/by/4.0/>



Open Access

---

## Abstract

It is generally accepted that the history of the expansion of the universe can be exactly described by the concordance model, which makes specific predictions about the shape of the Hubble diagram. The redshift-magnitude Hubble diagram in the redshift range  $z = 0.0104 - 1$  seems to confirm this expectation, and it is believed that this conformity is also valid in the high redshift range. However, this belief is not undisputed. Recent work in the high redshift range of up to  $z = 8.1$  has shown that the shape of the Hubble diagram deviates considerably from the predictions made by the Lambda cold dark matter model. These analyses, however, were based on mixed SN1a and gamma ray burst data, and some astronomers argue that this may have biased the results. In this paper, 109 cosmology-independent, calibrated gamma ray burst  $z/\mu$  data points are used to calculate the Hubble diagram in the range  $z = 0.034$  to  $z = 8.1$ . The outcome of this analysis confirms prior results: contrary to expectations, the shape of the Hubble diagram turns out to be exponential, and this is difficult to explain within the framework of the standard model. The cosmological implications of this unexpected result are discussed.

## Keywords

Redshift, Gamma Ray Bursts, Hubble Diagram, Exponential Slope, Hubble's Law,  $\Lambda$ CDM Model

---

## 1. Introduction

The basic premise of Big Bang cosmology is that the universe is expanding. Important evidence for this expansion is that it follows from general relativity (GR) [1], which has been successfully tested both in the solar system and on the cosmic scale.

Besides GR, the Hubble constant ( $H_0$ ) [2] is probably the most fundamental cosmological parameter. It is considered to be the most convincing evidence for universal expansion, and the universe expands with a velocity determined by the Hubble constant.

At the same time, however, we have to keep in mind that neither GR nor Hubble's constant is a real proof for expansion. GR when applied to the universe as a whole represents only a theoretical framework and allows the construction of numerous basically different cosmological models such as Einstein's static universe [1], the Einstein-deSitter model [3] and the dynamic, expanding or contracting, universe of Friedmann [4], for example. All these models are mathematically correct and none of them is preferred by GR. The presently prevailing inflationary  $\Lambda$ CDM model seems to confirm expansion and provides an excellent fit to most cosmological observations. However the price is high. The model rests on a large number of hypotheses, dark matter, dark energy, inflation, for example, which can either not be proved experimentally, or though theoretically provable, could not be proven, yet. Recently, a number of papers appeared in peer reviewed journals proposing new models without DM or DE or both [5] [6] [7] and without inflation [8].

And even the interpretation of Hubble's constant as recession velocity is hypothetical. Hubble never measured velocity; the expansion of the universe cannot be measured experimentally. The Hubble Law is a RS/distance relation, and the Hubble recession law is in reality a working hypothesis.

The question must be asked: how sure can we be that the universe really expands with velocity of the Hubble constant? Different tests based on observational data have been proposed to provide evidence for the expansion hypothesis. A critical review of these tests shows that convincing evidence for the universal expansion is still lacking [9] [10]. The static universe model fits the observational data better than expansion models [10] [11] [12].

A promising tool to confirm expansion is the Hubble diagram test. We expect that in the high RS range it should be possible to check more precisely whether the Hubble diagram follows the linear  $H_0 D/c$  (expanding models) or the exponential  $z+1 = e^{H_0 * t}$  (tired light) relation, an effect that is perceptible only slightly in the  $z < 1$  region. The Hubble diagram (HD), calculated on the basis of a SN1a supernovae redshift (RS,  $z$ )/magnitude ( $\mu$ ) data, gives an excellent fit to the predictions of the concordance model [13] [14] [15]. However, a hint of uncertainty remains. The fit of the Lambda cold dark matter model ( $\Lambda$ CDM) to the SN1a  $z/\mu$  data applies only within the narrow range of  $z = 0 - 1$ . One reason for this is experimental difficulties; at RSs  $> \sim 1.3$ , the optical light emitted by supernovae becomes increasingly dimmed with distance, probably due to gray dust extinction, and accurate observations become difficult. However, cosmologists are not concerned with this RS limitation and consider the RS range of  $z > \sim 1 - 8$  to be uninteresting. At higher RSs, the universe is matter-dominated, and the lambda term in the high RS region does not affect the universal expansion. It is

assumed that the HD at high RS would merely confirm the concordance cosmology [16]. In recent years, a number of papers appearing in peer-reviewed journals have drawn the conclusion that the shape of the HD is exponential over the entire RS range of 0.0104 - 8.1, in clear contrast to the specific predictions of the  $\Lambda$ CDM model [17] [18] [19]. These analyses were performed with mixed SN1a and gamma ray burst (GRB) data, and some astronomers argue that this may have biased the results.

The best way to confirm or disprove the exponential shape of the HD is to use exclusively GRB data to calculate the HD over the whole RS range of  $z = 0.034 - 8.1$ . In previous papers, several attempts have been made to utilize GRB data to calculate the HD [16] [20] [21] [22] [23] with varying degrees of success. The limited number of data points and the large scatter of the data do not allow for safe conclusions. However, thanks to Swift (The Neil Gehrels Swift Observatory, NASA), the main features of GRBs have become better known in recent years. On the basis of more accurate observations of GRBs, the expectation has arisen that these objects could prove to be suitable distance indicators. Many hundreds of bursts have been observed in the range  $0.034 < z \leq 8$ , which opens up the possibility of measuring the expansion history back to the formation of the first stars. It is expected that the maximum clearly observable RS could approach 10 or even larger. This could place significant constraints on the different models of universal expansion.

The aim of the present work is to perform an improved HD test based on a larger number of calibrated GRB RS/ $\mu$  data points. The reliability of these data was verified using statistical tests before the analysis was carried out.

## 2. Experimental

A total of 109 calibrated, cosmology independent GRB  $z/\mu$  data points collected by Wei [24] from the 557 Union2 compilations were used as the starting data set. From these 109 data points, three low RS data points 050416A ( $\mu = 41.44 \pm 1.2$ ), 080319B ( $\mu = 43.07 \pm 1.24$ ), 061121 ( $\mu = 46.18 \pm 1.01$ ), ( $\bar{\mu} = \pm 0.41$ ; average error in  $\mu$  for 50 low RS GRB data points) and three high RS data points 040912 ( $\mu = 43.27 \pm 2.06$ ), 09120 ( $\mu = 47.58 \pm 1.96$ ), and 080913 ( $\mu = 50.45 \pm 1.74$ ), ( $\bar{\mu} = \pm 1.55$ ; average error in  $\mu$  for 59 high RS GRB data points) were excluded from the following refinement process due to their unusually large error bars, which indicate observational difficulties in terms of magnitude determination.

For the remaining 103 data points, best fit curves were calculated, which are more accurate than those used in any previous work, using the empirical potential function

$$\mu = a * z^b, \quad (1)$$

with  $a = 44.1097$  and  $b = 0.05988$ , which was determined in earlier publications for SN1a gold set and for GRB data to be the best mathematical approximation for describing the slope of the  $z/\mu$  diagram [25] [26] [27].

## 2.1. Elimination of Outliers

In view of the experimental difficulties in determining the  $z/\mu$  data, it is likely that large data sets taken from different observations and from different sources will contain outliers. If these outliers are not removed from the refinement procedure, they will dominate the fit and bias the results.

## 2.2. Identification of Outliers: The Grubbs Test

The well-known Grubbs test [28] was used for the identification of erroneous luminosity indicators. The Grubbs test is used to detect outliers in a data set of  $N$  values that are nearly normally distributed. Assuming a normal distribution of the sample, as confirmed by the very low skew in **Table 1**, the test is performed by computing  $x_0$ , which is defined as:

$$X_0 \geq \frac{G_G * \text{STABW} + x_{\text{Mean}}}{\sqrt{\frac{N}{N-1}}} \quad (2)$$

where:

$x_0$  is the suspected outlier;

$x_{\text{Mean}}$  is the absolute value of the mean of the  $N$  data points;

$N$  is the number of data points;

STABW is the standard deviation of  $N$  values; and

$G_G$  is the Grubbs number.  $G_G$  can be found in statistical tables for different levels of confidence and numbers of data points. For 103 data points, for example,  $G$  is 1.956 at 95% confidence level.

If the  $x_0$  calculated from  $(\mu_{\text{measured}} - \mu_{\text{calculated}})$  is found to be greater than the numerical value of the right-hand side of Equation (1), the data point in question must be discarded; on the basis of the reduced data set, new  $a$  and  $b$  coefficients, the mean and the new STABW must be calculated, and so on.

## 2.3. Preparation of the Hubble Diagram

The Hubble diagram is a linear plot of the measured distance (usually Mpc) versus the measured RS, which is often represented on the less sensitive logarithmic  $\mu/\text{RS}$  scale.

Since the differences between the measured and the calculated trend lines become more pronounced on the linear scale, a plot of the photon flight time ( $t$ ) versus RS was used for representation of the HD. The photon flight time was calculated from

$$t = \frac{D}{c} = \frac{10^{(\mu+5)/5}}{(z+1) * 3 * 10^{10}} * 3.085 * 10^{18} \quad (3)$$

**Table 1.** Fit results from the starting data set. Descriptive statistics  $z/\mu$ .

Raw data	Valid cases	$a$	$b$	$R^2$	STABW $\mu_{\text{obs}} - \mu_{\text{calc}}$	Skew $\mu_{\text{obs}} - \mu_{\text{calc}}$
109	103	44.049	0.0595	0.9066	0.7384	0.4221

In Equation (2),  $t$  represents the flight time of the photons (in sec) from the co-moving radial distance  $D$  to the observer, which is proportional to  $D$  (Mpc) as used in the Hubble law.

## 2.4. Hubble Diagram Representation

The Hubble diagram as originally presented by Hubble [2] is a distance (Mpc)/velocity ( $v$ ) representation where  $v = cz$ . Recently it becomes increasingly common to use the logarithmic  $z/\mu$  diagram as presented in **Figure 1** and **Figure 2** instead of the linear distance/redshift scale.

The presentation  $t/(z + 1)$  as used in this paper is essentially equivalent to Hubble's depiction, with  $\text{Mpc} = t \times c$  (abscissa) and  $z = v/c$  (ordinate) and the two diagrams differ only in the scale of the axes. The advantage of the  $t/(z + 1)$  representation is, as can be seen in **Figure 3** and **Figure 4**, is that the slope of the best fit line can be fitted exactly with the exponential function  $z + 1 = e^{H_0 t}$ .

## 2.5. Luminosity Distances

Luminosity distances were calculated using the cosmological calculator described by Wright [29].

## 2.6. Excel and Excel Solver

Excel and Excel Solver were used for the data fitting, refinement, analysis and data presentation.

## 3. Results

The results of the fit procedure based on 103 raw data points are shown in **Figure 1** and **Table 1**.

As can be seen from **Figure 1**, the data are affected by considerable scatter, resulting in large variability of the data and a relatively poor goodness of fit indicator of  $R^2 = 0.9066$ .

A representative result of the iterative refinement process is shown in **Figure 2** and **Figure 3**. The corresponding descriptive statistics are summarized in **Tables 2-7**.

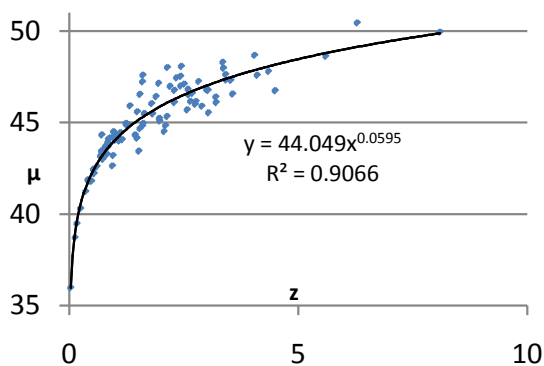


**Figure 1.** Best fit curve for the initial 103 GRB data points.

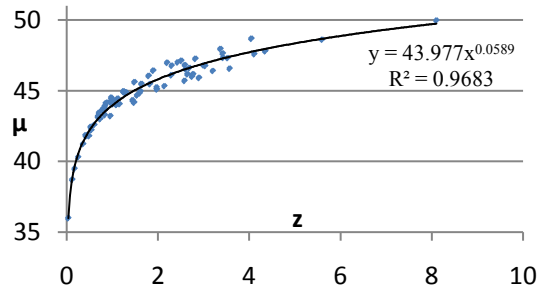


**Figure 2.** Best fit curve based on 84 statistically verified GRB  $z/\mu$  data points.

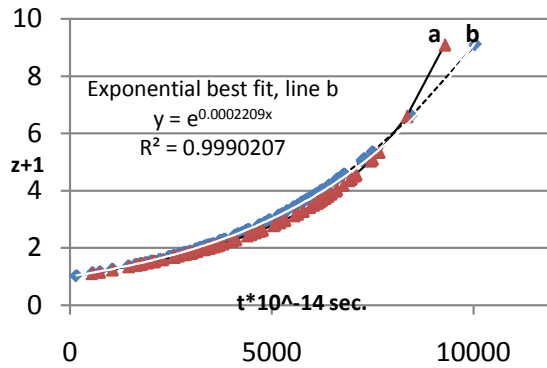


**Figure 3.** Representative Hubble diagram based on 84 statistically verified GRB  $z/\mu$  data points.

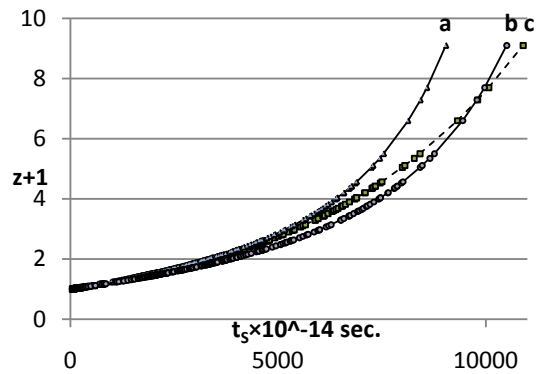


**Figure 4.** Redshift of type I a supernovae as a function of  $t = D_C/c$ . Squares (dashed line):  $t/z$  data inferred from the potential best-fit curve of the observed  $z/\mu$  diagram. Triangles:  $t/z$  relationship derived from the  $\Lambda$ CDM model with  $H_0 = 72.6 \text{ km}\cdot\text{s}^{-1}\cdot\text{Mpc}^{-1}$ , Circles:  $t/z$  relationship derived from the  $\Lambda$ CDM model with  $H_0 = 62.5 \text{ km}\cdot\text{s}^{-1}\cdot\text{Mpc}^{-1}$  (data are taken from [26]).

**Table 2.** Results of regression with  $\mu = a \times z^b$ . Descriptive statistics  $z/\mu$ , one iteration.

Valid cases	$a$	$b$	$R^2$	Variance ( $\mu_{\text{obs}} - \mu_{\text{calc}}$ )	$\Sigma\chi^2$ ( $\mu_{\text{obs}} - \mu_{\text{calc}}$ )
90	43.999	0.0592	0.9557	0.2538	0.4920
Mean ( $\mu_{\text{obs}} - \mu_{\text{calc}}$ )	Std. Deviation ( $\mu_{\text{obs}} - \mu_{\text{calc}}$ )	Error in Std. D.	Skew ( $\mu_{\text{obs}} - \mu_{\text{calc}}$ )	F-Test $\mu_{\text{obs}}/\mu_{\text{calc}}$	$P$
0.00073	0.5038	0.0531	0.0733	0.8281	1

**Table 3.** Results of regression. Descriptive statistics  $t/z + 1$ ; one iteration.

Valid cases	$H_0$		$R^2$	Variance ( $z_{\text{obs}} - z_{\text{calc}}$ )	$\Sigma\chi^2$ ( $z_{\text{obs}} - z_{\text{calc}}$ )
90	0.0002147 ( $2.147 \times 10^{-18} \text{ s}^{-1}$ )		0.99942	0.0032 ( $z_{\text{obs}} - z_{\text{calc}}$ )	0.099
Mean ( $z_{\text{obs}} - z_{\text{calc}}$ )	Std. Deviation ( $z_{\text{obs}} - z_{\text{calc}}$ )	Error in Std. D.	Skew ( $z_{\text{obs}} - z_{\text{calc}}$ )	F-Test $z_{\text{obs}}/z_{\text{calc}}$	$P$
0.0374	0.0569	0.006	1.028	0.7575	1

**Table 4.** Results of regression with  $\mu = a \times z^b$ . Descriptive statistics  $z/\mu$ ; two iterations.

Valid cases	$a$	$b$	$R^2$	Variance ( $\mu_{\text{obs}} - \mu_{\text{calc}}$ )	$\Sigma\chi^2$ ( $\mu_{\text{obs}} - \mu_{\text{calc}}$ )
84	43.977	0.0589	0.9683	0.181	0.3287
Mean ( $\mu_{\text{obs}} - \mu_{\text{calc}}$ )	Std. Deviation ( $\mu_{\text{obs}} - \mu_{\text{calc}}$ )	Error in Std. D.	Skew ( $\mu_{\text{obs}} - \mu_{\text{calc}}$ )	F-Test $\mu_{\text{obs}}/\mu_{\text{calc}}$	$P$
0.00158	0.4254	0.0464	-0.01075	0.8867	1

**Table 5.** Results of regression with  $t/z + 1$ . Descriptive statistics; two iterations.

Valid cases	$H_0$		$R^2$	Variance ( $z_{\text{obs}} - z_{\text{calc}}$ )	$\Sigma\chi^2$ ( $z_{\text{obs}} - z_{\text{calc}}$ )
84	0.0002209 ( $2.209 \times 10^{-18} \text{ s}^{-1}$ )		0.9990	0.0018	0.04279
Mean ( $z_{\text{obs}} - z_{\text{calc}}$ )	Std. Deviation ( $z_{\text{obs}} - z_{\text{calc}}$ )	Error in Std. D.	Skew ( $z_{\text{obs}} - z_{\text{calc}}$ )	F-Test ( $z_{\text{obs}}/z_{\text{calc}}$ )	$P$
0.00035	0.4255	0.0046	1.1519	0.8536	1

**Table 6.** Results of regression with  $\mu = a \times z^b$ . Descriptive statistics  $z/\mu$ ; three iteration.

Valid cases	$a$	$b$	$R^2$	Variance $\mu_{\text{obs}}/\mu_{\text{calc}}$	$\Sigma\chi^2$ $\mu_{\text{obs}}/\mu_{\text{calc}}$
80	43.976	0.0589	0.9732	0.1489	0.2593
Mean ( $\mu_{\text{obs}} - \mu_{\text{calc}}$ )	Std. Deviation ( $\mu_{\text{obs}} - \mu_{\text{calc}}$ )	Error in Std. D.	Skew ( $\mu_{\text{obs}} - \mu_{\text{calc}}$ )	F-Test $\mu_{\text{obs}}/\mu_{\text{calc}}$	$P$
0.001927	0.3859	0.0043	-0.174	0.9074	1

**Table 7.** Results of regression with  $t/z + 1$ . Descriptive statistics; three iteration.

Valid cases	$H$		$R^2$	Variance ( $z_{\text{obs}} - z_{\text{calc}}$ )	$\Sigma\chi^2$ ( $z_{\text{obs}} - z_{\text{calc}}$ )
80	0.0002208 ( $2.208 \times 10^{-18} \text{ s}^{-1}$ )		0.999	0.00176	0.03997
Mean ( $z_{\text{obs}} - z_{\text{calc}}$ )	Std. Dviation ( $z_{\text{obs}} - z_{\text{calc}}$ )	Error in Std. D.	Skew ( $z_{\text{obs}} - z_{\text{calc}}$ )	F-Test $z_{\text{obs}}/z_{\text{calc}}$	$P$
0.0007	0.042	0.0047	1.449	0.8549	1

(a) HD calculated on the basis of the currently most accurate LJA  $z/\mu$  data with best fit parameters  $H_0 = 70 \text{ km}\cdot\text{s}^{-1}\cdot\text{Mpc}^{-1}$ ,  $\Omega_m = 0.295$ ,  $w = -1.104$  [25]; (b)

measured best fit line. The results of the two iteration steps are shown in **Table 5**:

As can be seen from **Figure 3**, the shape of the HD is exponential or (more critically) very close to exponential, whilst the  $\Lambda$ CDM model shows systematic deviations from the exponential best fit curve ( $\Sigma\chi^2$  best fit, line  $b = 0.04279$ ;  $\Sigma\chi^2$   $\Lambda$ CDM model, line  $a = 0.3671$ ).

This result is in perfect agreement with earlier findings [18] that  $\Lambda$ CDM models show poor agreement with observation (**Figure 4**).

The HD diagram on basis of the  $\Lambda$ CDM model with  $H_0 = 62.5 \text{ km}\cdot\text{s}^{-1}\cdot\text{Mpc}^{-1}$  (line b in **Figure 3**) deviates below the trendline of the best-fit curve for  $z + 1 < 6.5$  to the bottom, and above it for  $z + 1 > 6.3$ . These deviations are of a non-statistical nature and thus the model does not reflect the observed exponential slope.

For  $H_0 = 72.6 \text{ km}\cdot\text{s}^{-1}\cdot\text{Mpc}^{-1}$  (line a in **Figure 4**) the  $\Lambda$ CDM model departs considerably from the observed exponential function (line c), and in the range  $z > \sim 2$ , a sharp increase is shown in the slope. A  $\Sigma\chi^2$  test shows a statistical significance between the observed  $t/\mu$  and the calculated  $\Lambda$ CDM data of  $P = 0.053$ , and fails to describe the observed  $z/\mu$  data completely.

**Tables 2-7** show that after only two iteration steps, the further removal of outliers does not result in a substantial improvement in terms of either shape or goodness of fit indicators.

#### 4. Discussion

The results presented here show that the Hubble diagram  $t/(z + 1)$  calculated on the basis of GRB  $z/\mu$  data follows a strictly exponential slope in the range  $0.0331 < z < 8.1$ , in excellent agreement with observation. The exponential slope of the Hubble diagram provides a clear indication of an energy decrease in the emitted spectral lines with a constant rate. At RSs  $> \sim 2$ , the  $\Lambda$ CDM model does not fit the data well (dashed line in **Figure 3**). This unexpected result leads to a logical contradiction between theory and observation, which cannot be solved within the frame of the concordance model. We consider it certain that the universe (spacetime) expands, and the expanding space causes a RS in the photons that is proportional to the extent of expansion. The shape of the HD should follow the explicit predictions of the concordance model, which cannot be exponential.

The question arises of how to interpret these contradictory results in light of the expansion hypothesis. If we exclude the static universe model, the most radical answer explaining this disagreement would be that something is wrong with the basic assumptions of the underlying cosmological model. The results presented here require that the HD is completely determined by an energy decay process that is as yet unknown, which most cosmologists are not ready to accept, since this would require the most important evidence for universal expansion to be discarded.

It is not the aim of this paper to identify a specific new energy decay mechan-

ism (although some promising alternatives have been proposed in the recent literature [26] [27] [30] [31] to explain these contradictory results); however, it should be pointed out that the disagreement between the predictions of the concordance model and the strictly exponential slope of the HD is a real problem that requires an explanation. In view of this, the HD test may prove to be the most important cross check in determining the expansion history of the universe and the physical meaning of  $H_0$ . Increasingly accurate high-RS GRB  $z/\mu$  data may turn out to be the key to this important cosmological issue. There is hope this could be done in the near future.

“We are now at an interesting juncture in cosmology. With new methods and technology, the accuracy in measurement of the Hubble constant (from high RS GRB data) has vastly improved, but a recent tension has arisen that is signaling as-yet unrecognized uncertainties. The key pillar of the standard cosmological model becomes shaky” [32] [33].

### Conflicts of Interest

The author declares no conflicts of interest regarding the publication of this paper.

### References

- [1] Einstein, A. (1917) Kosmologische Betrachtungen zur allgemeinen Relativitätstheorie, Sitzungsberichte der Königlich Preußischen Akademie der Wissenschaften (Berlin), S. 142-152. [Cosmological Observations about the General Theory of Relativity, Proceedings of the Royal Prussian Academy of Sciences, Vol. 142-152.]
- [2] Hubble, E.P. (1929) A Relation between Distance and Radial Velocity among Extra-Galactic Nebulae. *Proceedings of the National Academy of Sciences of the United States of America*, **15**, 167-173. <https://doi.org/10.1073/pnas.15.3.168>
- [3] Einstein, A. and deSitter, W. (1932) On the Relation between the Expansion and the Mean Density of the Universe. *Proceedings of the National Academy of Sciences of the United States of America*, **18**, 213-214. <https://doi.org/10.1073/pnas.18.3.213>
- [4] Friedmann, A. (1922) Über die Krümmung des Raumes. *Zeitschrift für Physik*, **10**, 377-386. <https://doi.org/10.1007/BF01332580>
- [5] Moffat, J.W. and Toth, V.T. (2012) Modified Gravity: Cosmology without Dark Matter or Einstein’s Cosmological Constant. arXiv:0710.0364v7[astro-ph]
- [6] Mitra, A. (2011) An Astrophysical Peek into Einstein’s Static Universe, No Dark Energy. *International Journal of Astronomy and Astrophysics*, **1**, 183-199. <https://doi.org/10.4236/ijaa.2011.14024>
- [7] Mitra, A. (2013) Energy of Einstein’s Static Universe and Its Interpretation for the  $\Lambda$ CDM Cosmology. *International Journal of Cosmology and Astroparticle Physics*, No. 3, Article ID: 007.
- [8] Mitra, A. (2014) Why the Big Bang Model Does Not Allow Inflationary and Cyclic Cosmologies though Mathematically One Can Obtain Any Model with Favorable Assumptions. *New Astronomy*, **30**, 46-50. <https://doi.org/10.1016/j.newast.2013.12.002>
- [9] López-Corrediora, M. (2017) Tests and Problems of the Standard Model in Cosmology. *Foundations of Physics*, **47**, 711-768.

- <https://doi.org/10.1007/s10701-017-0073-8>
- [10] Lerner, E.J. (2018) Observation Contradict Galaxy Size and Surface Brightness Predictions That Are Based on the Expanding Universe Hypothesis. *MNRAS*, **477**, 3185-3196. <https://doi.org/10.1093/mnras/sty728>
- [11] Lòpez-Corrediora, M. (2018) Problems with the Dark Matter and Dark Energy Hypothesis, and Alternative Ideas. arXiv: 1808.09823
- [12] Crawford, D.A. (2011) Observational Evidence Favors a Static Universe. *The Journal of Cosmology*, **13**, 3875-3946.
- [13] Perlmutter, S., *et al.* (1999) Measurements of  $\Omega$  and  $\Lambda$  from 42 High-Redshift Supernovae. *The Astrophysical Journal*, **517**, 565-586. <https://doi.org/10.1086/307221>
- [14] Riess, A., *et al.* (1998) Observational Evidence from Supernovae for an Accelerating Universe and a Cosmological Constant. *Astronomical Journal*, **116**, 1009-1038. <https://doi.org/10.1086/300499>
- [15] Schmidt, B.P., *et al.* (1994) The Expanding Photosphere Method Applied to SN 1992am AT CZ = 14600 km/s. *Astronomical Journal*, **107**, 1444-1452. <https://doi.org/10.1086/116957>
- [16] Schäfer, B.E. (2006) The Hubble Diagram to Redshift > 6 from 69 Gamma-Ray Bursts. arXiv:astro-ph/0612285
- [17] Marosi, L.A. (2013) Hubble Diagram Test of Expanding and Static Cosmological Models: The Case for a Slowly Expanding Universe. *Advances of Astronomy*, **2013**, Article ID: 917104. <https://doi.org/10.1155/2013/917104>
- [18] Marosi, L.A. (2014) Hubble Diagram Test of 280 Supernovae Redshift Data. *Journal of Modern Physics*, **5**, 29-33. <https://doi.org/10.4236/jmp.2014.51005>
- [19] Marosi, L.A. (2016) Modelling and Analysis of the Hubble Diagram of 280 Supernovae and Gamma Ray Bursts Redshifts with Analytical and Empirical Redshift/Magnitude Data. *International Journal of Astronomy and Astrophysics*, **6**, 272-275. <https://doi.org/10.4236/ijaa.2016.63022>
- [20] Izzo, L., Capozziello, S., Covone, G. and Capaccioli, M. (2009) Extending the Hubble Diagram by Gamma Ray Bursts. *Astronomy and Astrophysics*, **508**, 63-67. <https://doi.org/10.1051/0004-6361/200912769>
- [21] Demianski, M., Piedipalumbo, E. and Rubano, C. (2011) The Gamma-Ray Bursts Hubble Diagram in Quintessential Cosmological Models. *Monthly Notices of the Royal Astronomical Society*, **411**, 1213-1222. <https://doi.org/10.1111/j.1365-2966.2010.17751.x>
- [22] Cardone, V.F., Capozziello, S. and Dainotti, M.G. (2009) An Updated Gamma Ray Bursts Hubble Diagram. arXiv: 0901.3194v2
- [23] Liu, J. and Wei, H. (2015) Cosmological Models and Gamma-Ray Bursts Calibrated by Using Padé Method. *General Relativity and Gravitation*, **47**, 141. <https://doi.org/10.1007/s10714-015-1986-1>
- [24] Wei, H. (2010) Observational Constraints on Cosmological Models with the Updated Long Gamma Ray Bursts. *Journal of Cosmology and Astroparticle Physics*, **2010**, 14. <https://doi.org/10.1088/1475-7516/2010/08/020>
- [25] Betoule, M., *et al.* (2014) Improved Cosmological Constraints from a Joint Analysis of the SDSS-II and SNLS Supernova Samples. *Astronomy & Astrophysics*, **568**, Article No. A22. arXiv:1401.4064 <https://doi.org/10.1051/0004-6361/201423413>
- [26] Marosi, L.A. (2017) Is the Velocity Interpretation of the Redshift of Spectral Lines in Accordance with Astronomical Data? *International Journal of Astronomy and*

---

*Astrophysics*, **7**, 248-254. <https://doi.org/10.4236/ijaa.2017.74021>

- [27] Lineweaver, C.H. and Barbosa, B. (1998) Cosmic Microwave Background: Implications for Hubble Constant and the Spectral Parameters  $n$  and  $Q$  in Cold Dark Matter Critical Density Universes. *Astronomy & Astrophysics*, **329**, 799-808.
- [28] Grubbs, E. (1950) Sample Criteria for Testing Outlying Observations. *The Annals of Mathematical Statistics*, **21**, 27-58. <https://doi.org/10.1214/aoms/1177729885>
- [29] Wright, E.I. (2006) A Cosmology Calculator for the World Wide Web. *Publications of the Astronomical Society of the Pacific*, **118**, 1711-1715. <https://doi.org/10.1086/510102>
- [30] Blanchard, A., Douspis, M., Rowan-Robinson, M. and Sarkar, S. (2003) An Alternative to the Cosmological “Concordance Model”. *Astronomy & Astrophysics*, **412**, 35-44. <https://doi.org/10.1051/0004-6361:20031425>
- [31] Marosi, L.A. (2017) Non Velocity Interpretation of the Cosmic Redshift—Cosmological Implications. <http://gsjournal.net/Science-Journals/ResearchPapers-Cosmology/Download/6954>
- [32] Friedmann, W.L. (2017) Cosmology at a Crossroads: Tension with the Hubble Constant. *Nature Astronomy*, **1**, 0169. arXiv: 1706.02739
- [33] Nielsen, J.T., Guffanti, A. and Sarkar, S. (2016) Marginal Evidence for Cosmic Acceleration from Type Ia Supernovae. *Scientific Reports*, **6**, Article No. 35596. <https://doi.org/10.1038/srep35596>